PNAS RESEARCH ARTICLE | GENETICS OPEN ACCESS

FETCH enables fluorescent labeling of membrane proteins in vivo with spatiotemporal control in *Drosophila*

Kevin D. Rostam[a,b,c], Nicholas C. Morano[a,b,d], Kaushiki P. Menon[c], Davys H. Lopez[b,e], Lawrence Shapiro[a,b,d], Kai Zinn[c], Siqian Feng[a,b,1], and Richard S. Mann[a,b,f,g,2]

Affiliations are included on p. 11.

Edited by Claude Desplan, New York University, New York, NY; received February 11, 2025; accepted August 24, 2025

Fluorescent labeling approaches are crucial for elucidating protein function and dynamics. While robust methods to monitor gene transcription are widespread, the visualization of proteins in vivo is more elusive. To meet this challenge, we developed Fluorescent Endogenous Tagging with a Covalent Hook (FETCH) to label cell surface proteins (CSPs) in vivo through a stable covalent bond mediated by the DogTag-DogCatcher peptide partner system. FETCH leverages a spontaneous covalent isopeptide bond that forms between the 23-amino acid DogTag and the 15-kDa DogCatcher. Unlike most tags that work best at protein termini, DogTag functions well in protein loops, expanding the range of sites that can be targeted in proteins. In FETCH, DogTag is introduced into extracellular loops of CSPs through genome engineering, enabling covalent bond formation with a genetically encoded DogCatcher-GFP fusion protein that can be secreted from a variety of cell types in intact animals. To identify optimal DogTag insertions into CSPs, we describe a flow cytometry–based platform for rapidly screening candidates in vitro. We demonstrate the ability to tag and visualize three members of the immunoglobulin superfamily (IgSF) in vivo: the transmembrane protein mCD8 and two GPI-anchored proteins belonging to the DIP-Dpr interactome that interact biophysically to facilitate neuronal target recognition at *Drosophila* neuromuscular and brain synapses. FETCH enables precise temporal and spatial control to visualize tagged proteins in vivo, features that are adaptable to a multitude of applications for modifying any cell surface protein.

cell adhesion molecules | protein tagging | protein subcellular localization | axon guidance | synapse specificity

Significance

Animal nervous systems require that neurons make the correct connections during development. Neuronal target recognition is facilitated by cell surface proteins (CSPs), localized to opposing membranes, that interact biophysically through extracellular domains. Here, we describe FETCH, a method for the fluorescent labeling of CSPs in vivo mediated by covalent bond formation between two peptides, DogTag and DogCatcher. CSPs with DogTag insertions recruit endogenously expressed DogCatcher that is fused to fluorescent proteins, enabling protein-specific visualization with temporal and spatial control. Importantly, we demonstrate that covalent bond formation does not interfere with interactions and functionality of two *Drosophila* CSP partners, DIP-α and Dpr10. FETCH lays the groundwork for the labeling of other membrane proteins, enabling a host of previously unfeasible applications.

The ability to visualize and perturb proteins in vivo is critical for understanding how they function within cells. Labeling proteins generally depends on their ability to tolerate the addition of fluorescent tags or small epitopes, most typically at their termini (1). While some proteins are amenable to modification, a large number of protein families are challenging to tag, hindering the use of conventional approaches. A prominent example are the DIPs (Dpr interacting proteins) and Dprs [Defective in Proboscis Extension Response (2)], members of the immunoglobulin superfamily (IgSF) in *Drosophila melanogaster*. The interaction network of DIPs and Dprs was first characterized by an extracellular domain interaction assay for *Drosophila* cell surface proteins (CSPs) (3). Further work has demonstrated that interactions between DIPs and Dprs facilitate neuronal target recognition and subsequent synaptogenesis in many tissues at multiple developmental stages (4–14). The well-characterized interaction between DIP-α and Dpr10 is required for the stabilization of neuromuscular junctions (NMJs) in both the larva and adult, where neuronal DIP-α interacts with Dpr10 molecules localized to the muscle cell membrane. In the larval neuromuscular system, genetic knockout of *DIP-α* or *dpr10* results in failed muscle innervation and mistargeting events by specific motor neuron axons (15–17). Similarly, both *DIP-α* and *dpr10* are required for a subset of motor neurons to recognize and innervate their stereotyped muscles in the adult leg after successful navigation to these targets (18–20).

The DIPs and Dprs consist of three and two immunoglobulin-like (Ig) domains, respectively, at their N termini. The binding interface for DIP-Dpr interactions occurs between the most membrane-distal, N-terminal Ig1 domains of both proteins (4, 21). At their C termini, both sets of proteins are tethered to the cell membrane via a glycosylphosphatidylinositol (GPI) anchor (22). During translation and after entry into the endoplasmic reticulum, a C-terminal fragment of GPI-anchored proteins is cleaved at residues comprising the so-called ω-site, after which the mature protein is covalently bound to a GPI moiety and trafficked to the cell membrane (23). These structural constraints make the termini of DIPs and Dprs unavailable for modification, impeding the ability of standard labeling techniques

The authors declare no competing interest.

This article is a PNAS Direct Submission.

[1]Present Address: The Key Laboratory of Developmental Genes and Human Disease, The School of Life Sciences and Technology, Southeast University, Nanjing 210096, China.

[2]To whom correspondence may be addressed. Email: rsm10@columbia.edu.

This article contains supporting information online at https://www.pnas.org/lookup/suppl/doi:10.1073/pnas.2503166122/-/DCSupplemental.

Published October 15, 2025.

that typically depend on tagging protein termini, such as affinity tags and fluorescent proteins, to visualize these molecules.

Due to these limitations, we developed a method based on DogTag-DogCatcher technology that we term "Fluorescent Endogenous Tagging with a Covalent Hook" (FETCH). This technology takes advantage of the loop-friendly DogTag-DogCatcher system, which enables spontaneous covalent bond formation between proteins (24). The 23-amino acid DogTag peptide rapidly and spontaneously forms a covalent isopeptide bond with a specific binding partner, a 15-kDa protein denoted as DogCatcher (24). The orthologous SpyTag-SpyCatcher pair, designed for ligation at protein termini, has previously been applied in vivo to tag transcription factor termini for chromatin immunoprecipitation (25). Unlike SpyTag's β strand conformation that does not work well in protein loops, DogTag has a β hairpin structure that is more compatible with insertion into these regions, making it an optimal candidate for introduction into CSPs to mediate the covalent fusion with other proteins (24).

We identify optimal DogTag insertion sites for DIP-α, Dpr10, and, for comparison, the transmembrane mouse CD8 (mCD8) protein, by using an easily scalable flow cytometry–based platform. CSPs with DogTag insertions are expressed on the surface of mammalian cells grown in culture, where ligation efficiency with DogCatcher can be quantitatively evaluated. We perform coupling reactions using recombinant expression of the most efficient DogTag variants of each CSP to biochemically confirm covalent bond formation. To study the localization of these proteins in vivo, we established lines with optimized DogTag insertions and used DogCatcher-GFP to fluorescently label DIP-α, Dpr10, and mCD8 with temporal control at *Drosophila* neuromuscular junctions and brain synapses. We also generated a set of reagents that provide a secreted source of DogCatcher-GFP from a variety of cell types. The ability to rapidly identify optimal DogTag insertion sites in conjunction with the ease of genetic implementation positions FETCH as a versatile tool for protein-specific tagging and functional studies.

Results

Overview of FETCH. In FETCH, a DogTag is introduced into the extracellular domains of CSPs of interest (Fig. 1*A*). In addition to DIP-α and Dpr10, we also introduce DogTag into mCD8, a mouse lymphocyte protein widely used as a membrane-localized marker of neuronal processes in *Drosophila* (26). Vertebrate CD8 is also a member of the immunoglobulin superfamily (IgSF) class of CSPs, and contains a single Ig-like domain in both CD8α and CD8β subunits (27). Unlike DIPs and Dprs, CD8 is anchored to the membrane via a single-pass transmembrane domain. To facilitate colocalization studies in vivo, we fused an mCherry fluorescent protein to mCD8α's intracellular C terminus (mCD8-mCherry). To identify suitable DogTag insertion sites in CSPs, we used a flow cytometry–based platform to quantify ligation efficiency between DogCatcher and a range of DogTag insertions into DIP-α, Dpr10, and mCD8-mCherry (Fig. 1*B*). This platform allows for the screening of large numbers of insertion sites in native membrane environments without necessitating recombinant protein production, making this approach readily scalable and adaptable to any CSP. In vivo, the 104-amino acid DogCatcher

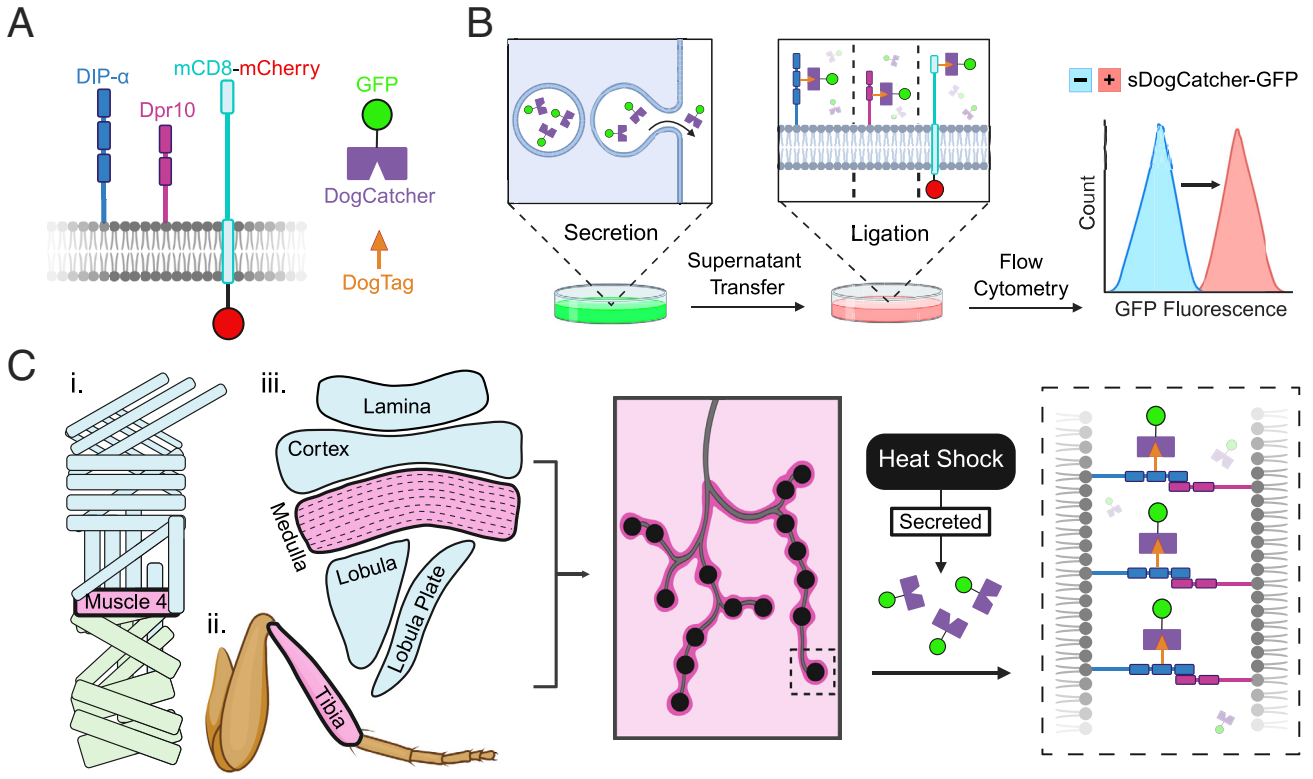

Fig. 1. Overview of FETCH and flow cytometry platform for identifying successful DogTag insertion sites. (*A*) Schematic of FETCH components including the DogTag peptide, secreted DogCatcher fused to moxGFP (sDogCatcher-GFP), and the cell surface proteins (CSPs) of interest, which in this study are the IgSF proteins DIP-α, Dpr10, and mCD8. (*B*) Workflow for identifying optimal DogTag insertions. Transfection of an sDogCatcher-GFP encoding plasmid into HEK293 cells results in fusion protein secretion into the supernatant. The medium is transferred to HEK293 cells expressing membrane-localized DogTag variants of DIP-α, Dpr10, or mCD8. Flow cytometry is used to quantify the efficiency of covalent bond formation between DogTag candidates and sDogCatcher-GFP. (*C*) In this study, DogTagged-CSPs localized to i) larval or ii) adult neuromuscular junctions and iii) pupal optic lobe neuropils are labeled by sDogCatcher-GFP, which is expressed using an inducible heat shock promoter and secreted extracellularly. When in proximity to a DogTag-CSP, a spontaneous covalent bond between DogTag and DogCatcher forms, enabling protein-specific fluorescent labeling in vivo. The pink regions contain neural synapses examined in later figures.

is genetically encoded with a C-terminal fusion to a fluorescent protein and an N-terminal signal sequence to facilitate secretion. Its expression is regulated by a heat shock-inducible promoter (*hsp70*) to allow temporal control over labeling of DogTag-CSPs in a variety of tissue types (Fig. 1*C*).

Flow Cytometry Quantifies the Ligation Efficiency of DogTag Insertions into CSPs. A variety of DogTag insertion sites were tested using our flow cytometry platform for all three proteins. For DIP-α and Dpr10, DogTag insertion into the N-terminal Ig1 domain of both proteins was avoided to prevent disrupting the binding interface required for their interaction [PDB: 6NRQ (4)] (Fig. 2*E*). Based on available crystal structures (4, 27), we targeted loops in the more membrane-proximal Ig domains of DIP-α (Ig2 and Ig3) and Dpr10 (Ig2), and in the sole Ig domain of the mCD8-mCherry fusion protein. We also inserted DogTags in the regions C-terminal to Ig3 for DIP-α or Ig2 for Dpr10, preceding the predicted sites of GPI linkage (20). We refer to these regions as membrane linkers, which AlphaFold 3 (28) predicts to be unstructured (*SI Appendix*, Fig. S1 *B* and *D*). For mCD8-mCherry, the loops of its Ig domain, the unstructured membrane linker region, and a site immediately following its N-terminal signal peptide were targeted (*SI Appendix*, Fig. S1*F*). In all cases, the 23-amino acid DogTag was flanked on both sides with a flexible five amino acid glycine-serine linker (*Materials and Methods*).

A total of nine, three, and eight independent DogTag insertions were screened for DIP-α, Dpr10, and mCD8-mCherry, respectively. To assess covalent bond formation between DogTag-CSPs and DogCatcher, full-length tagged CSP variants were transfected into HEK293 Freestyle cells. Expression levels were evaluated by monitoring cytoplasmic mCherry, which was expressed using the IRES system for DIP-α and Dpr10, and as a C-terminal fusion for mCD8-mCherry. We selected the cysteine-less moxGFP for fusion to DogCatcher, which is monomeric and engineered for use in the secretory pathway (29). Recombinant DogCatcher-moxGFP, engineered with the secrecon signal peptide that drives robust secretion in mammalian cells (30), was harvested from conditioned medium following transfection (*Materials and Methods*). Secreted DogCatcher-moxGFP (here on referred to as sDogCatcher-GFP) was incubated with cells expressing DogTag-CSPs, which were then washed and assessed for DogTag-DogCatcher ligation by flow cytometry with green fluorescence as the readout. For each CSP, multiple DogTag

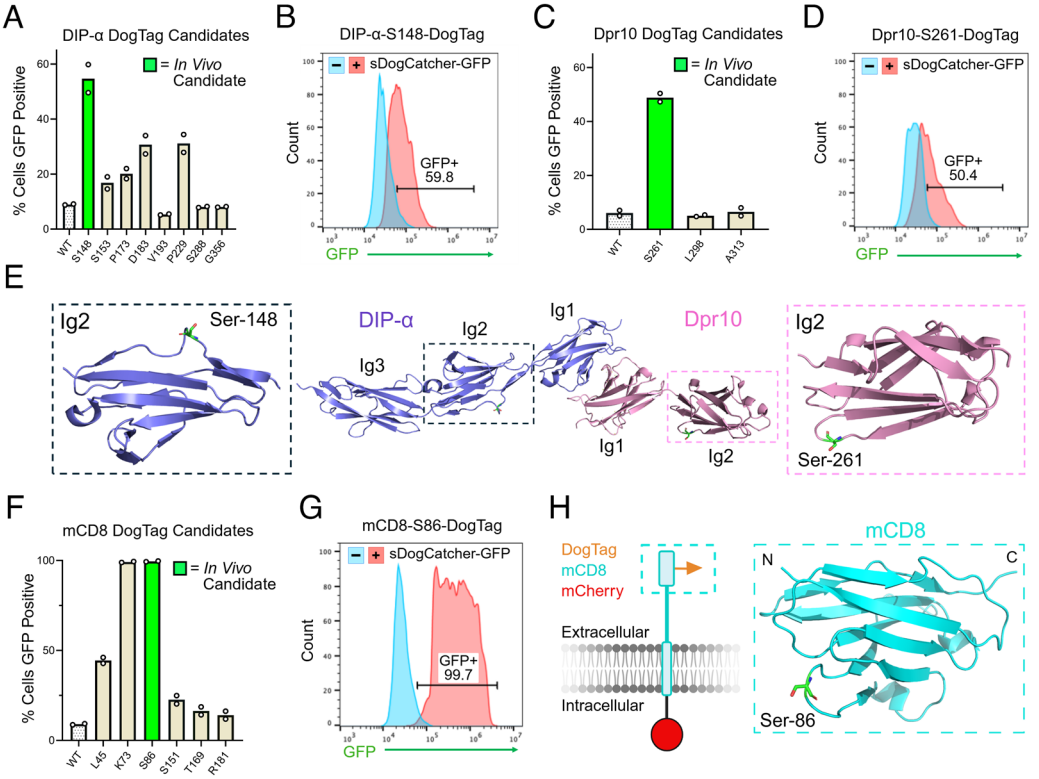

Fig. 2. Flow cytometry quantifies the efficacy of covalent bond formation of DogTag insertion sites in DIP-α, Dpr10, and mCD8 in vitro. (*A*) Bar graph showing flow cytometry quantification of covalent bond formation between sDogCatcher-GFP and DogTag candidates cloned into Ig2, Ig3, and the membrane linker region of DIP-α. Loop insertion of DogTag after residue Ser148 for DIP-α produced the largest fluorescent signal as detected by flow cytometry. (*B*) Histogram plot displaying change in fluorescent signal when supernatant containing sDogCatcher-GFP is incubated with HEK293 cells transfected with DIP-α-Ser148-DogTag (red peak) compared to cells incubated without sDogCatcher-GFP (blue peak). (*C*) Bar graph showing flow cytometry quantification of covalent bond formation between sDogCatcher-GFP and DogTag candidates cloned into Ig2 and the membrane linker region of Dpr10. Loop insertion of DogTag after residue Ser261 for Dpr10 produced the largest fluorescent signal as detected by flow cytometry. (*D*) Histogram plot displaying change in fluorescent signal when supernatant containing sDogCatcher-GFP is incubated with HEK293 cells transfected with Dpr10-Ser261-DogTag (red peak) compared to cells incubated without sDogCatcher-GFP (blue peak). (*E*) Crystal structure representation of the interaction between binding partners DIP-α and Dpr10 (PDBID: 6NRQ) (4). DogTag insertion sites at Ser148 and Ser261 for DIP-α and Dpr10, respectively, are indicated. (*F*) Bar graph showing flow cytometry quantification of covalent bond formation between sDogCatcher-GFP and DogTag candidates cloned into the sole Ig domain and membrane linker region of mCD8. Loop insertion of DogTag after residue Ser86 for mCD8 produced the largest fluorescent signal as detected by flow cytometry. (*G*) Histogram plot displaying change in fluorescent signal when supernatant containing sDogCatcher-GFP is incubated with HEK293 cells transfected with mCD8-Ser86-DogTag (red peak) compared to cells incubated without sDogCatcher-GFP (blue peak). (*H*) Schematic of mCD8-DogTag-mCherry, where DogTag is inserted into the Ig domain and mCherry is fused to the truncated cytoplasmic domain. Crystal structure of mCD8's Ig domain (PDBID: 2ATP) (27) with the DogTag insertion site at Ser86 is indicated. DogTag flanked with flexible linkers was inserted immediately after the indicated residue numbers in all constructs. Flow experiments were run in duplicate for all constructs. *WT* = Wildtype versions of respective CSPs without DogTag. An increase in fluorescence indicates covalent bond formation between DogTag-CSPs and sDogCatcher-GFP (*B*, *D*, and *G*). FACS analysis of other DogTag-CSP variants and negative control WT proteins without DogTag are shown in *SI Appendix*, Fig. S1.

variants demonstrated coupling with sDogCatcher-GFP (*SI Appendix*, Fig. S1 *A*, *C*, and *E*). Among the DIP-α candidates, DogTag insertion into Ig2 after Ser148 achieved the largest fluorescent signal (Fig. 2 *A* and *B*). Of the Dpr10 candidates, DogTag insertion into Ig2 after Ser261 produced the largest signal (Fig. 2 *C* and *D*). For mCD8-mCherry, DogTag insertions into the Ig domain after Lys73 and Ser86 demonstrated the largest signals (Fig. 2 *F* and *G*). Based on these results, DIP-α-S148-DogTag, Dpr10-S261-DogTag, and mCD8-S86-DogTag were identified as the most efficient variants and were selected for all subsequent biochemical and in vivo experiments (Fig. 2 *E* and *H*). For simplicity, below we refer to these variants as DIP-α-DogTag, Dpr10-DogTag, and mCD8-DogTag-mCherry.

Tagged Loops Achieve Efficient Protein–Protein Coupling In Vitro. We compared the coupling efficiency of loop-optimized DogTag-DogCatcher to SpyTag003-SpyCatcher003, a highly efficient orthologous system for ligation at protein termini (31). For these experiments, the extracellular domains of DIP-α-DogTag (Ig1-Ig3), Dpr10-DogTag (Ig1-Ig2), and mCD8-DogTag-mCherry (sole Ig), were fused to a hemagglutinin (HA) signal peptide at their N termini and SpyTag003 and 8xHis at their C termini. Transfection of these expression constructs into Expi293 suspension cells resulted in protein secretion into medium, which was purified and concentrated for biochemistry. DogCatcher-GFP and SpyCatcher003 proteins were obtained by standard bacterial expression and purification. DIP-α-DogTag-SpyTag003-8xHis, Dpr10-DogTag-SpyTag003-8xHis, and mCD8-DogTag-SpyTag003-8xHis were independently incubated with either DogCatcher-GFP or SpyCatcher003 (Fig. 3*A*). Coupling reactions for all three CSP fragments resulted in prominent bands equivalent to the expected molecular weight of the ligation product for both DogTag-DogCatcher and SpyTag003-SpyCatcher003 coupling (Fig. 3 *B*–*D*). Importantly, bands due to DogTag-mediated ligation in protein loops achieve comparable efficiency to SpyTag-mediated ligation at termini, revealing that DogTag-DogCatcher ligation is also highly efficient.

FETCH Enables Labeling of CSPs at the Larval Neuromuscular Junction In Vivo. We generated a transgene in which expression of sDogCatcher-GFP is under the control of the heat shock-inducible *hsp70* promoter, allowing for temporally controlled expression in all cells (Fig. 4*A*). To boost the signal, we fused DogCatcher to 6 tandem copies of moxGFP (sDogCatcher-6xGFP), which resulted in a much stronger signal than a fusion with only 1 copy of moxGFP (*SI Appendix*, Fig. S3). We also generated a transgene in which the *hsp70* promoter and sDogCatcher-6xGFP coding region were separated by a Flippase (Flp)-deletable FRT>STOP>FRT cassette, which we use below to restrict the secretion of sDogCatcher-6xGFP to specific cells. We verified secretion of DogCatcher in vivo by driving excision

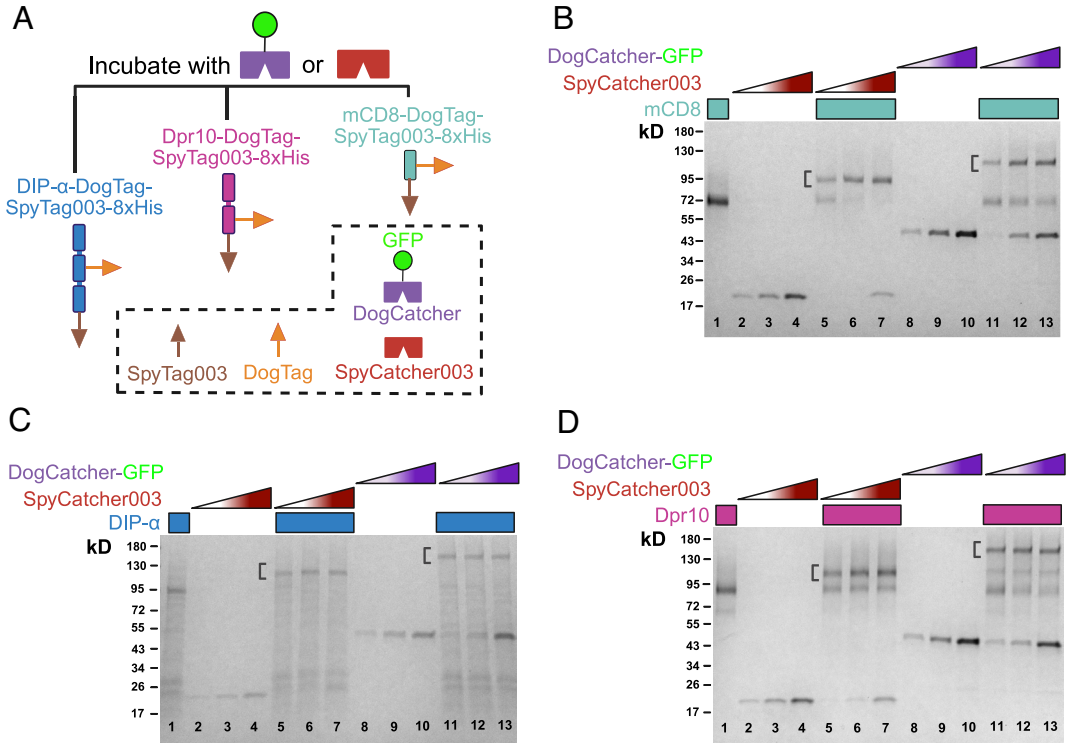

Fig. 3. DogTag couples to DogCatcher with high efficiency in protein loops of DIP-α, Dpr10, and mCD8. (*A*) Schematic showing soluble versions of DIP-α-DogTag, Dpr10-DogTag, and mCD8-DogTag that were generated by truncating their membrane linker regions, leaving Ig-like domains only. As a positive control for covalent bond formation, all three soluble protein variants were fused to a C-terminal SpyTag003, known to couple to SpyCatcher003 with high efficiency (31). Soluble protein variants were incubated with increasing concentrations of DogCatcher-GFP or SpyCatcher003 in neutral buffer for 1 h at room temperature. (*B*) SDS-PAGE with approximately 5 pmols of mCD8-DogTag-SpyTag003-8xHis loaded in lanes 1, 5–7, and 11–13. DogCatcher-GFP or SpyCatcher003 amounts vary from half equimolar, equimolar, to twice equimolar relative to mCD8 in lanes 2–4, 5–7, 8–10, and 11–13, as indicated. Bands due to DogTag-DogCatcher coupling in lanes 11–13 have a similar efficiency to bands due to SpyTag003-SpyCatcher003 coupling in lanes 5–7. The molecular weight marker is shown on the *Left*. (*C*) SDS-PAGE with approximately 2.5 pmols of DIP-α-DogTag-SpyTag003-8xHis loaded in lanes 1, 5–7, and 11–13. DogCatcher-GFP or SpyCatcher003 amounts vary from half equimolar, equimolar, to twice equimolar relative to DIP-α in lanes 2–4, 5–7, 8–10, and 11–13, as indicated. Bands due to DogTag-DogCatcher coupling in lanes 11–13 have a similar efficiency to bands due to SpyTag003-SpyCatcher003 coupling in lanes 5–7. The molecular weight marker is shown on the *Left*. (*D*) SDS-PAGE with approximately 5 pmols of Dpr10-DogTag-SpyTag003-8xHis loaded in lanes 1, 5–7, and 11–13. DogCatcher-GFP or SpyCatcher003 amounts vary from half equimolar, equimolar, to twice equimolar relative to Dpr10 in lanes 2–4, 5–7, 8–10, and 11–13, as indicated. Bands due to DogTag-DogCatcher coupling in lanes 11–13 have a similar efficiency to bands due to SpyTag003-SpyCatcher003 coupling in lanes 5–7. The molecular weight marker is shown on the *Left*. Brackets indicate protein bands resulting from DogTag-DogCatcher or SpyTag003-SpyCatcher003 ligation (*B*, *C*, and *D*).

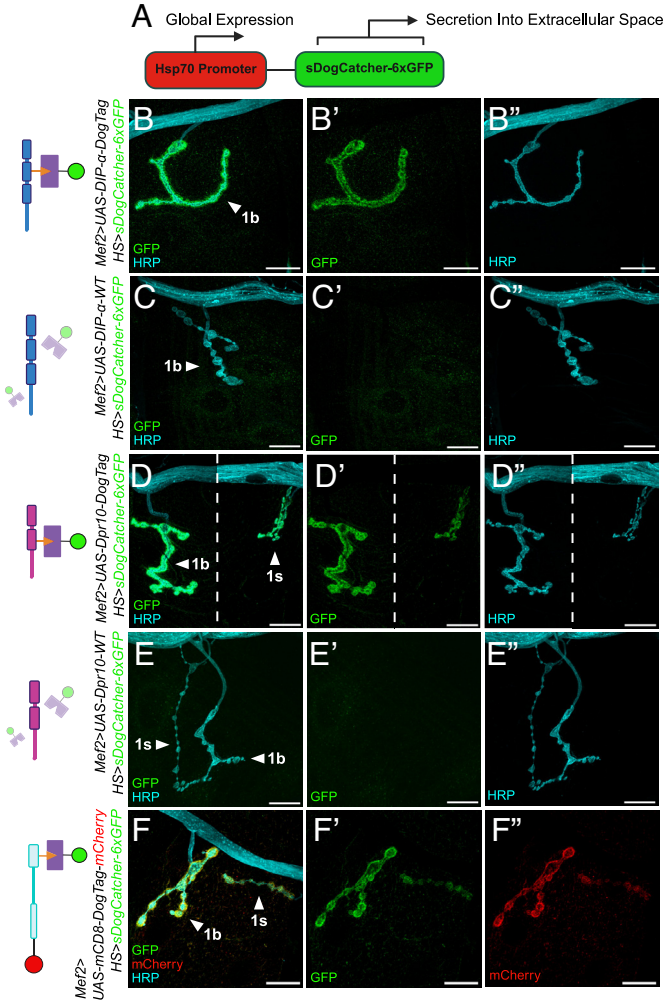

Fig. 4. FETCH enables fluorescent labeling of DogTag-CSPs in vivo. (*A*) Schematic demonstrating global expression of sDogCatcher-6xGFP, under the temporal control of the *hsp70* promoter. sDogCatcher-6xGFP secretion from all cells is achieved via standard heat shock. (*B*, *B*′, and *B*″) *Mef2-Gal4* drives expression of DIP-α-DogTag in third instar larval muscles, which localizes to the subsynaptic reticulum (SSR) of NMJs, as detected by ligation with global expression of sDogCatcher-6xGFP. A single confocal slice of Type 1b boutons at muscle 4 (m4) is shown as merged (*B*), GFP only (*B*′), and HRP only (*B*″) images. As observed previously (17), the absence of the 1s bouton is a consequence of *cis* inhibition, when DIP-α is overexpressed in muscles. (*C*, *C*′, and *C*″) Mef2-Gal4 drives expression of DIP-α-WT in third instar larval muscles. Heat shock-induced sDogCatcher-6xGFP secretion occurs in the absence of a DogTag binding partner, with no detectable m4 SSR signal. A single confocal slice of Type 1b boutons at m4 is shown as merged (*C*), GFP only (*C*′), and HRP only (*C*″) images. As observed previously (17), the absence of the 1s bouton is a consequence of *cis* inhibition, when DIP-α is overexpressed in muscles. (*D*, *D*′, and *D*″) *Mef2-Gal4* drives expression of Dpr10-DogTag in third instar larval muscles, which localizes to the SSR of NMJs, as detected by ligation with global expression of secreted sDogCatcher-6xGFP. A single confocal slice of Type 1b and Type 1s boutons at m4 is shown as merged (*D*), GFP only (*D*′), and HRP only (*D*″) images. (*E*, *E*′, and *E*″) Mef2-Gal4 drives expression of Dpr10-WT in third instar larval muscles. Heat shock-induced sDogCatcher-6xGFP secretion occurs in the absence of a DogTag binding partner, with no detectable m4 SSR signal. A single confocal slice of Type 1b and Type 1s boutons at m4 is shown as merged (*E*), GFP only (*E*′), and HRP only (*E*″) images. (*F*, *F*′, and *F*″) Mef2-Gal4 drives expression of mCD8-DogTag-mCherry in third instar larval muscles, which localizes to the SSR of NMJs, as detected by ligation with global expression of sDogCatcher-6xGFP. A single confocal slice of Type 1b and Type 1s boutons is shown as merged (*F*), GFP only (*F*′), and mCherry only (*F*″) images. Arrowheads call out synaptic bouton types (*B*–*F*). Dashed lines denote separate focal planes within the same lateral plane (*D*). (All scale bars, 20 μm.)

of the stop cassette in the *hsp70>STOP>sDogCatcher-6xGFP* transgene with Hedgehog-Gal4; UAS-Flp, allowing for heat shock-inducible expression only in the posterior compartment of the wing imaginal disc, and observed GFP fluorescence in the apical lumen of the anterior compartment (*SI Appendix*, Fig. S2*A*). Identical heat shock conditions in the absence of Flp expression produced no signal, suggesting that there is no transcriptional read-through of the stop cassette (*SI Appendix*, Fig. S2*A*). When mCD8-DogTag-mCherry is expressed in a subset of neurons in the larval ventral nerve cord, heat shock-induced global expression of sDogCatcher-6xGFP results in robust labeling only in the cells that express the tagged protein (*SI Appendix*, Fig. S3 *A*–*D*). Thus, these experiments confirm that DogTagged proteins can be recognized and bound in vivo by secreted sDogCatcher-6xGFP.

As a second test of FETCH, we used global heat shock-induced expression of sDogCatcher-6xGFP to label DIP-α-DogTag and Dpr10-DogTag when overexpressed at the larval neuromuscular junction (NMJ) using the muscle Gal4 driver, *Mef2-Gal4*. In both cases, we observe a robust GFP signal at the subsynaptic reticulum (SSR), invaginations of the muscle membrane that envelop 1b (big) and 1s (small) boutons, two types of glutamatergic motor neurons in the larval neuromuscular system (32) (Fig. 4 *B* and *D*). Notably, no signal was observed when untagged DIP-α-WT and Dpr10-WT were similarly overexpressed in the presence of global sDogCatcher-6xGFP expression (Fig. 4 *C* and *E*). We also obtained robust labeling of mCD8-DogTag-mCherry in both 1b and 1s boutons when expressed with *Mef2-Gal4* (Fig. 4*F*). For these and all subsequent NMJ experiments using heat shock-induced expression of sDogCatcher-6xGFP, we found that a 30 min heat shock, followed by a ~12 h chase prior to dissection, achieved an optimal signal over background, and without any aggregation of GFP (*SI Appendix*, *Extended Methods*). Together, these experiments demonstrate that overexpressed DogTag-CSPs can be successfully coupled to DogCatcher at neuromuscular junctions in vivo.

Cell Type–Specific Enhancers Provide Spatial Control Over DogCatcher-GFP Expression. The experiments described above all rely on the *hsp70* promoter to drive temporally controlled, but ubiquitous expression of sDogCatcher-6xGFP. To provide spatial as well as temporal control over sDogCatcher-6xGFP secretion, we generated multiple *enhancer-Flp* transgenes to drive Flippase expression and restrict secretion to specific cell types (Fig. 5*A*). Based on previously described *enhancer-Gal4* transgenes, we chose enhancers with activity specific to immature myocytes (*Him-Flp*), mature myoblasts (33) (*Mhc-Flp*), fat body (34) (*3.1Lsp2-Flp*), glia (35) (*Repo-Flp*), and both hemocytes and fat body (36) (*Cg-Flp*). We confirmed their activity and cell-type specificity by staining pupae, using an *actin>STOP>GFP* transgene as our readout (*SI Appendix*, Fig. S2*B*). In the larval NMJ, a glial source of sDogCatcher-6xGFP (*Repo-Flp; hsp70>STOP>sDogCatcher-6xGFP*) successfully labeled mCD8-DogTag-mCherry when expressed in the MNISN-1s glutamatergic motor neuron with DIP-α-Gal4 (Fig. 5*B*). Here, labeling is observed in both the 1s bouton and the MNISN-1s axon, suggesting that the extracellular DogTag in mCD8 can be ligated to glia-derived sDogCatcher-6xGFP during trafficking in axons (Fig. 5*B*′). Labeling is undetectable in the absence of a Flp source (Fig. 5*C*).

Next, we screened the ability of these cell type–restricted sources of sDogCatcher-6xGFP (*enhancer-Flp; hsp70>STOP>sDogCatcher-6xGFP*) to label mCD8-DogTag-mCherry in the adult leg NMJ. mCD8-DogTag-mCherry was expressed by DIP-α-Gal4, which is active in a subset of leg motor neurons (18). Cytoplasmic mCherry reporter expression was included to unambiguously visualize the DIP-α-Gal4-expressing motor neurons. We observed the strongest signal at the leg NMJ when sDogCatcher-6xGFP was secreted from muscles and hemocytes, compared to fat body and glia (Fig. 5*D* and *SI Appendix*, Fig. S4). While we present labeling of the motor neuron targeting the long tendon muscle of the tibia in adult T1 legs

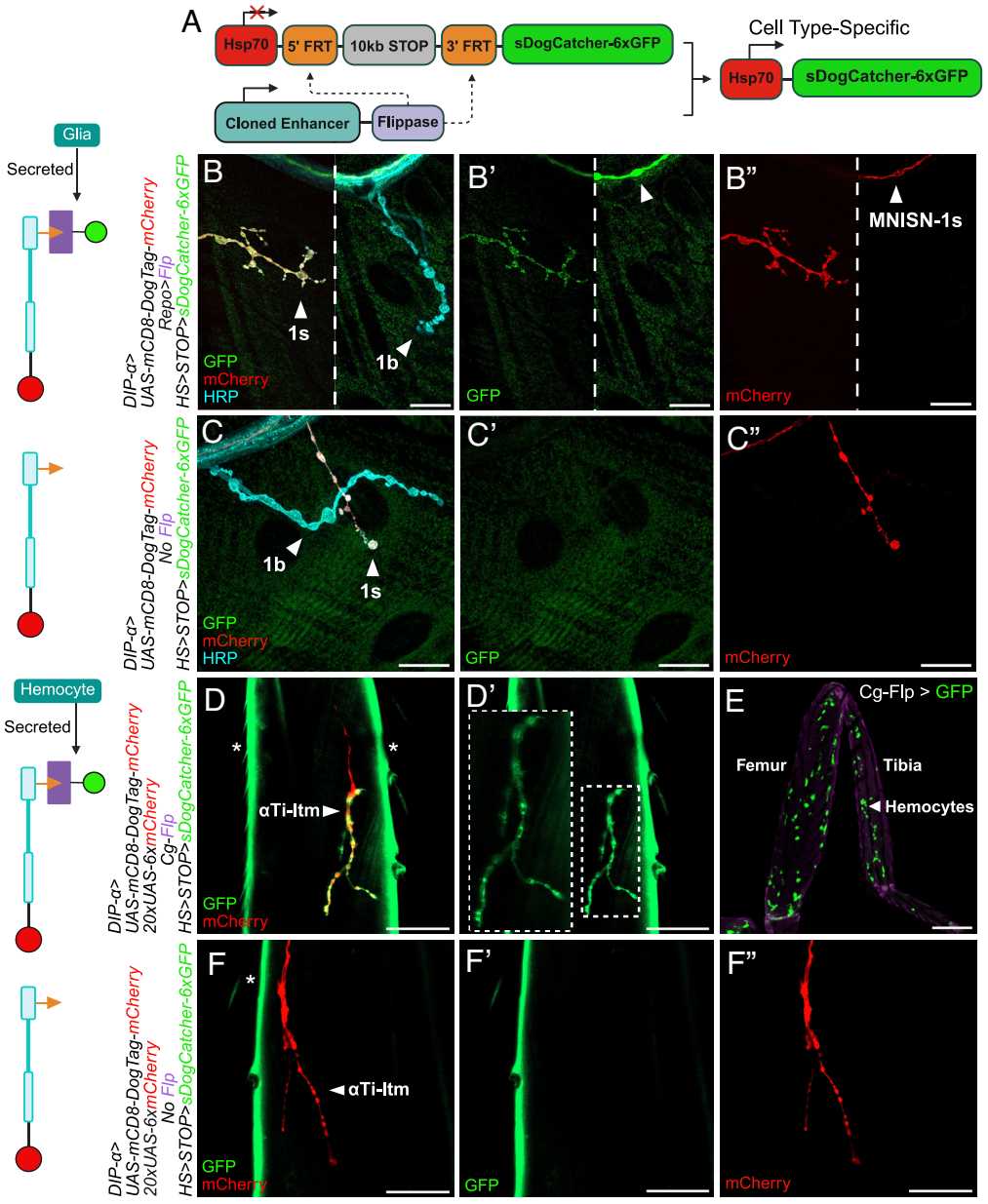

Fig. 5. FETCH enables temporal and spatial control over fluorescent labeling in a cell type–specific manner. (*A*) Schematic demonstrating a spatially restricted paradigm. Cell type–specific enhancers directly drive Flp expression, which excises an FRT-flanked stop cassette between *hsp70* and the sDogCatcher-6xGFP coding sequence, enabling temporal heat shock-inducible expression with cell type–specificity. (*B*, *B*′, and *B*″) *DIP-α-Gal4* drives neuronal expression of mCD8-DogTag-mCherry in the MNISN-1s neuron that innervates larval muscle 4 (m4). Note that GFP and mCherry signals are also observed in the nerve (arrowheads, *B*′ and *B*″). *Repo-Flp* deletes the FRT-flanked stop cassette to enable heat shock-induced sDogCatcher-6xGFP secretion from glial cells. A single confocal slice is shown as merged (*B*), GFP only (*B*′), and mCherry only (*B*″) images. (*C*, *C*″ and *C*″) *DIP-α-Gal4* drives neuronal expression of mCD8-DogTag-mCherry in the MNISN-1s neuron that innervates m4. Heat shock in the absence of a Flippase (Flp) source prevents stop cassette excision, transcriptionally terminating sDogCatcher-6xGFP expression. A single confocal slice is shown as merged (*C*), GFP only (*C*′), and mCherry only (*C*″). (*D* and *D*′) *DIP-α-Gal4* drives neuronal expression of mCD8-DogTag-mCherry in the motor neuron targeting the long tendon muscle of the tibia in adult T1 legs (αTi-ltm). *DIP-α-Gal4* also drives cytoplasmic mCherry reporter expression. *Cg-Flp* deletes the FRT-flanked stop cassette to enable heat shock-induced sDogCatcher-6xGFP secretion from hemocytes. A single confocal slice is shown as merged (*D*) and GFP only (*D*′) images. Asterisks denote cuticle autofluorescence (*D*). Contrast of sDogCatcher-6xGFP localization is enhanced in inset (*D*′). (*E*) Constitutive *Cg-Flp* expression deletes an FRT-flanked stop cassette between a constitutive actin promoter and Gal4 coding sequence, driving cytoplasmic GFP reporter expression in hemocytes in an adult T1 leg. Arrowhead calls out GFP-positive hemocytes. (*F*, *F*′, and *F*″) *DIP-α-Gal4* drives neuronal expression of mCD8-DogTag-mCherry in the αTi-ltm motor neuron in the adult T1 leg. *DIP-α-Gal4* also drives cytoplasmic mCherry reporter expression. Heat shock in the absence of a Flp source prevents stop cassette excision, transcriptionally terminating sDogCatcher-6xGFP expression. A single confocal slice is shown as merged (*F*), GFP only (*F*′), and mCherry only (*F*″). Asterisk denotes cuticle autofluorescence (*F*). Arrowheads call out synaptic bouton types (*B*–*D*, and *F*). Dashed lines denote separate focal planes within the same lateral plane (*B*). [Scale bars, 20 μm (*B* and *C*), 25 μm (*D* and *F*), and 100 μm (*E*).]

(αTi-ltm), we also observed strong labeling of all *DIP-α* expressing motor neurons in the tibia and femur. For labeling adult leg NMJs, *Cg-Flp*, which is restricted to hemocytes in the adult leg, emerged as the best nonneuronal and nonmuscle source of sDogCatcher-6xGFP (Fig. 5*E*). Labeling of the leg NMJ is undetectable in the absence of a Flp source (Fig. 5*F*). Taken together, these experiments demonstrate that nonneuronal and nonmuscle sources of sDogCatcher-6xGFP can successfully label extracellular domains of CSPs at neuromuscular junctions.

FETCH Enables Visualization of DIP-α and Dpr10 at Endogenous Levels With Single-Cell Resolution. All of the above experiments rely on Gal4-UAS-driven expression of DogTagged CSPs, which

can result in nonphysiological expression levels and aberrant localization of these proteins. To determine whether FETCH can label CSPs expressed at endogenous levels, CRISPR-Cas9 was used to introduce the DogTags described above for both DIP-α and Dpr10 at their native loci (Fig. 6*A*). We tested the ability of these proteins to be labeled at the larval NMJ, where innervation of the MNISN-1s motor neuron onto muscle 4 (m4) requires both DIP-α and Dpr10, expressed in the 1s motor neuron and SSR of m4, respectively (17). Following heat shock-induced expression of sDogCatcher-6xGFP, we observe labeling of DIP-α-DogTag at the boutons of 1s neurons, but not 1b neurons, which do not express DIP-α (Fig. 6*B*). GFP labeling of tagged DIP-α is also observed in the MNISN-1s axon, suggesting that FETCH can label CSPs as they are trafficking in axons (Fig. 6*B*). Importantly, identical heat shock conditions in the absence of a DogTag-CSP demonstrate no promiscuous tagging in synaptic boutons of m4 and the MNISN-1s axon (Fig. 6*D*). For endogenously expressed Dpr10-DogTag, heat shock-induced expression of sDogCatcher-6xGFP labeled the SSRs enveloping both 1s and 1b boutons of m4 (Fig. 6*C*). Interestingly, the signal was stronger in the 1s boutons that have a less extensive SSR compared to 1b boutons, consistent with the idea that Dpr10 is stabilized by the presence of DIP-α, which is expressed in 1s, but not 1b motor neurons (21, 37). We also observed labeling of DIP-α-DogTag and Dpr10-DogTag at muscle 3 and muscle 2, which the MNISN-1s neuron also innervates. These results reveal that FETCH can be used to resolve protein-specific localization at the cellular level.

DogTag-DogCatcher Ligation Does Not Disrupt the Function of DIP-α and Dpr10. For FETCH to be a valuable tool, the covalent bond formed between the DogTag-CSP and sDogCatcher-6xGFP should not interfere with the function of the tagged protein of interest. The innervation frequency of MNISN-1s onto m4 has been extensively characterized as being highly sensitive to changes in the expression levels of both DIP-α and Dpr10 (17). We find that *DIP-α-DogTag* and *dpr10-DogTag* homozygous animals, both with and without the expression of sDogCatcher-6xGFP, have a 1s innervation frequency comparable to wildtype animals without tagged DIP-α or Dpr10 (Fig. 6*E*). These results provide strong evidence that the function of these CSPs is not compromised by either DogTag insertions or after their ligation with sDogCatcher-6xGFP. Based on these findings, we posit that DogTag-DogCatcher ligation can be used to fluorescently visualize CSPs without compromising biophysical interactions and functions in vivo.

FETCH Detects Population-Level Endogenous Expression of DIP-α and Dpr10 in the Developing Optic Lobe. Last, we tested whether FETCH labels endogenous levels of DIP-α and Dpr10 in other parts of the nervous system, namely the pupal optic lobe where their pairwise interaction is well described (6, 15). DIP-α is expressed in multicolumnar interneurons Dm1, Dm4, and Dm12 in the medulla (21) while Dpr10 is broadly expressed in many lamina neurons including L3 and L5 (6, 15) (Fig. 7*A*). Morphology of these cells (38) and their connectivity patterns within the layers of the medulla have been described (6), where Dm1 and L5 serve as synaptic partners in the M1 layer while both Dm4 and Dm12 serve as synaptic partners to L3 in the M3 layer (Fig. 7*A*). Using FETCH to label DIP-α-DogTag with heat shock-derived sDogCatcher-6xGFP reveals prominent fluorescence in putative M1 and M3 layers at 27 h APF. These layers are marked with the axon terminals of R8 and R7 photoreceptors that target these temporary layers at this stage of development (Fig. 7*B*) (39). By 45 h APF, DIP-α-DogTag-positive Dm1, Dm4, and Dm12 processes can be visualized in M1 and M3 medullary layers (Fig. 7 *C* and *D*). The visualization of DIP-α in these layers, and the relative positions of R8 and R7 photoreceptors that temporarily occupy distal M1 and M5 layers respectively, is consistent with reported expression patterns at this stage (6, 39). At both 27 h and 45 h APF, Dpr10-DogTag labeling with FETCH is coincident with the layers labeled by DIP-α-DogTag (compare Fig. 7 *B* and *C* with *G* and *H*). M1 and M3 layers are distinctly labeled by Dpr10-DogTag at 45 h APF, indicative of the L3 and L5 lamina neuron processes that synapse onto DIP-α expressing neurons (Fig. 7*I*). As with our NMJ experiments, GFP fluorescence was not detected when identical heat shock conditions were used to express sDogCatcher-6xGFP in the absence of tagged DIP-α or Dpr10 at both timepoints (Fig. 7 *E* and *F*). We also found that the strength of the FETCH signal can be significantly amplified by using an anti-GFP antibody, without increasing background signal (*SI Appendix,* Fig. S5).

In the central brain, we also observed specific DIP-α-DogTag labeling at endogenous levels within the protocerebral bridge in the central complex at both 27 h and 50 h APF (*SI Appendix*, Fig. S6 *A* and *B*). Based on the dimensions and breadth of this labeling, it appears that DIP-α expression is likely present in many of the eighteen glomeruli within this tissue (40). We did not observe labeling of Dpr10-DogTag (*SI Appendix*, Fig. S6*C*), and similarly did not observe nonspecific labeling in the absence of DogTagged alleles (*SI Appendix*, Fig. S6*D*).

Discussion

Fluorescent labeling approaches are critical for revealing protein localization and dynamics in vivo. FETCH overcomes several major limitations of existing techniques. For one, the use of a streamlined flow cytometry–based platform enables rapid identification and quantitative evaluation of DogTag insertion sites into membrane-localized CSPs in vitro, greatly accelerating the rate at which tagged CSP libraries can be screened. Further, unlike other methods, FETCH facilitates fluorescent tagging through a single DogTag insertion into a protein loop. The DogTag is subsequently covalently bound by DogCatcher variants expressing a variable number of GFP copies that can be tuned to the expression levels of the CSP of interest. Two alternative in vivo labeling approaches in *Drosophila* depend on split-fluorescent protein tags that reconstitute fluorescence (41) or the recognition of epitope tags by nanobodies (42). These techniques typically rely on the insertion of tandem repeats of tags to enhance detectability, demanding larger structural modifications to the CSP. Another approach uses cell type–specific allele knock-ins of entire fluorescent proteins or, if the expression level is sufficient, small tags in a scarless manner (43). There are also several approaches for sparse labeling of CSPs. For example, one approach relies on intronic MiMIC gene traps to introduce whole fluorescent proteins into gene loci in the wrong orientation, which are then stochastically reoriented through the expression of a tissue-specific recombinase (44). Another promising method to achieve sparse labeling uses cell type–specific expression of recombinases to express epitope-tagged CSPs (45). While these methods are generally limited to proteins that can tolerate cytoplasmic epitopes, intersecting a recombinase-based approach with FETCH holds significant and generalizable promise to achieve sparse labeling of many CSPs. Since protein loops are abundant in extracellular domains, FETCH can be harnessed to label both GPI-linked as well as transmembrane proteins in the immunoglobulin superfamily (IgSF) and other structural families of CSPs. FETCH is also able to rely on an entirely endogenous signal without exogenous amplification with antibodies or nanobodies, though these measures can be implemented

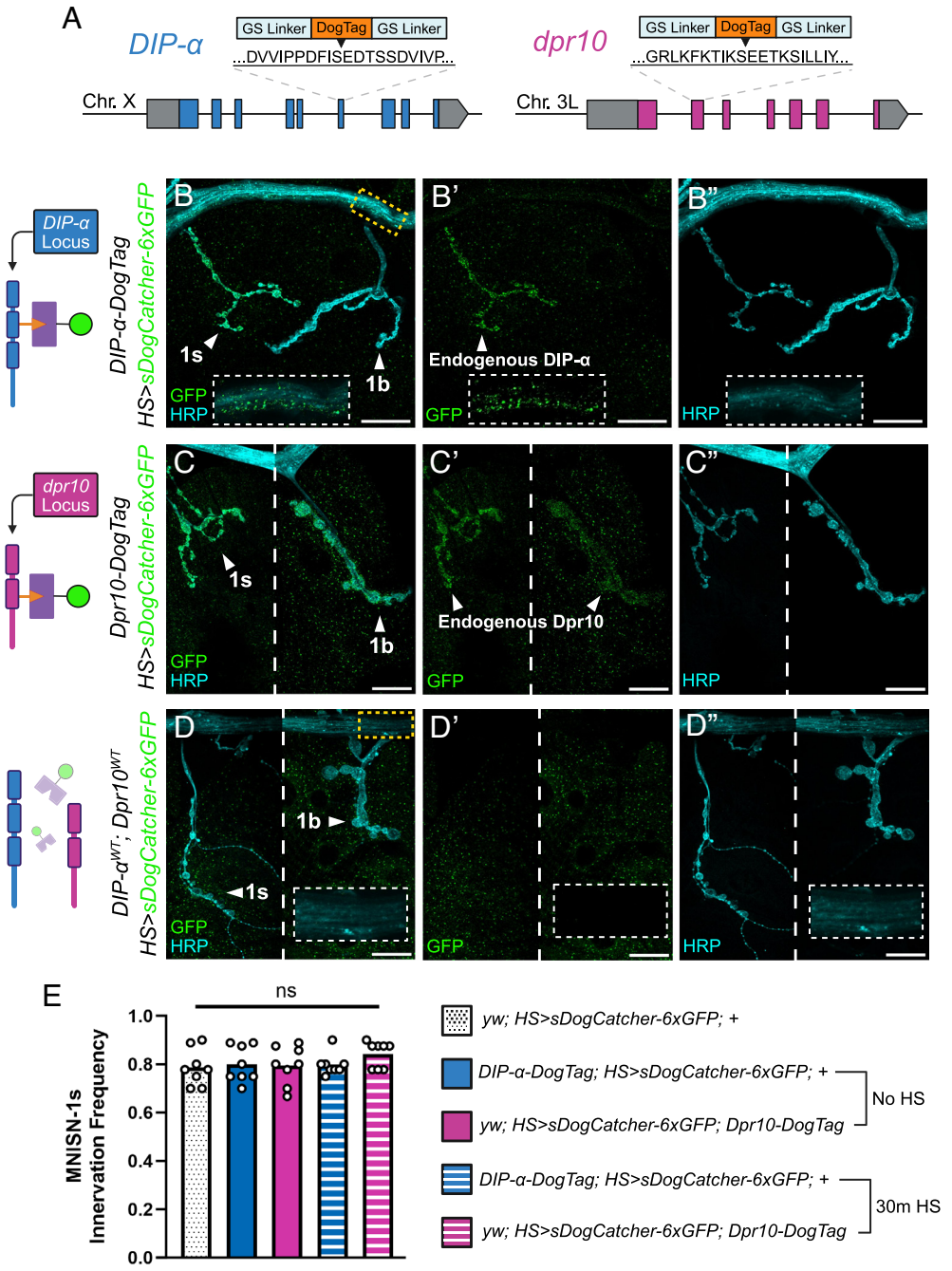

Fig. 6. FETCH achieves fluorescent labeling of DIP-α and Dpr10 at endogenous expression levels at neuromuscular junctions. (*A*) Schematic denoting locations of CRISPR-Cas9 mediated insertion of DogTag at the endogenous loci of *DIP-α* and *dpr10*. Gray boxes denote 5′ and 3′ UTRs. Colored boxes denote exons. Black lines denote introns. (*B*, *B*′, and *B*″) Homozygous DIP-α-DogTag expressed at endogenous levels localizes to 1s boutons innervating third instar larval muscle 4 (m4), as detected by ligation to global expression of sDogCatcher-6xGFP. A single confocal slice is shown as merged (*B*), GFP only (*B*′), and HRP only (*B*″) images. White dashed insets magnify the region contained within the yellow dashed box (*B*) and show active trafficking of DIP-α-DogTag in the MNISN-1s nerve. GFP and HRP signals in magnified insets are contrast enhanced. (*C*, *C*′, and *C*″) Homozygous Dpr10-DogTag expressed at endogenous levels localizes to the subsynaptic reticulum (SSR) surrounding 1s and 1b boutons innervating m4, as detected by ligation to heat shock-induced expression of sDogCatcher-6xGFP. A single confocal slice is shown as merged (*C*), GFP only (*C*′), and HRP only (*C*″) images. (*D*, *D*′, and *D*″) Heat shock-induced sDogCatcher-6xGFP expression with wildtype DIP-α and Dpr10 alleles does not result in promiscuous labeling in the absence of DogTag. White dashed insets magnify the region contained within the yellow dashed box (*D*) and demonstrates no signal in the nerve. (*E*) Quantitative comparison reveals no significant difference in MNISN-1s innervation frequency of third instar larval m4 in the presence of DIP-α-DogTag and Dpr10-DogTag alleles, both with and without ligation to heat shock-induced expression of sDogCatcher-6xGFP. Each datapoint represents the averaged % innervation frequency of multiple hemisegments in an individual animal. (Animals/Hemisegments) of genotypes in descending order of legend = (8/75), (8/67), (8/72), (8/75), (8/69). Abdominal hemisegments in A2 to A6 were quantified for all animals. Genetic knockout of both DIP-α and Dpr10 results in total loss of MNISN-1 s innervation of m4 (17). *WT* = Wildtype proteins without DogTag. Arrowheads call out synaptic bouton types (*B*–*D*). Contrast enhancement of GFP and HRP signals in magnified insets (*B* and *D*) was performed consistently across samples and with the same confocal slices of respective figures. (All scale bars, 20 μm.) Imaging and innervation frequency was determined in animals homozygous for all endogenous alleles and transgenes.

(*SI Appendix*, Fig. S5). This fully endogenous strategy enables protein labeling in tissues, such as the adult leg with its cuticle, that are difficult to access with exogenous reagents.

Surprisingly, in flow cytometry experiments, we observed that all DogTag insertions into the membrane linker regions (predicted to be unstructured) of all three CSPs (DIP-α-G356-DogTag,

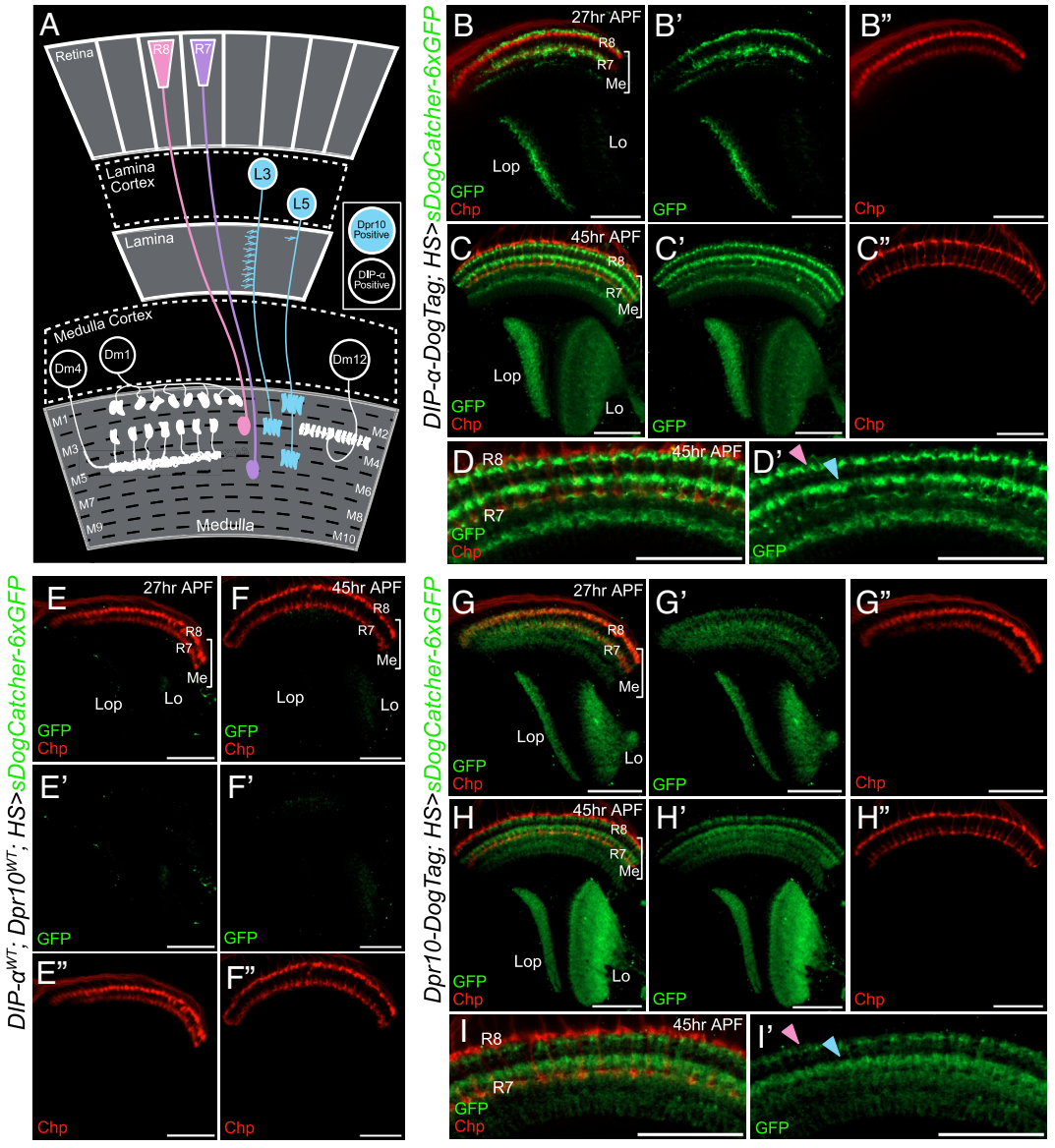

Fig. 7. FETCH labels endogenous levels of DIP-α and Dpr10 during pupal optic lobe development. (*A*) Schematic describing DIP-α-positive distal medulla (Dm) cells, Dpr10-positive lamina (L) cells, and inner photoreceptor cells in the adult optic lobe. DIP-α-positive cells in the medulla cortex terminate at layers M1 (Dm1), M3 (Dm4), and M3 (Dm12) in the medulla neuropil. Dpr10-positive cells in the lamina cortex receive input in the lamina and terminate at layers M3 (L3) and M1, M2, and M5 (L5) in the medulla neuropil. R8 and R7 photoreceptors project from the retina and pass through the lamina to terminate at M3 and M6 layers in the medulla neuropil, respectively. (*B*, *B*′, and *B*″) Homozygous DIP-α-DogTag expressed at endogenous levels localizes to putative M1 and M3 medullary layers and in the lobula plate at 27 h after puparium formation (APF), as detected by ligation to global expression of sDogCatcher-6xGFP. A single confocal slice is shown as merged (*B*), GFP only (*B*′), and Chaoptin (Chp) only (*B*″) images. Chp labels R8 and R7 photoreceptor axons, thus serving as a marker for layers M3 and M6, respectively. (*C*, *C*′, and *C*″) Homozygous DIP-α-DogTag expressed at endogenous levels localizes to M1, M3, and one additional layer in the distal medulla (layers M1 to M6 in panel *A* schematic). Labeling is also observed in an additional layer in the proximal medulla (layers M8-10), lobula, and lobula plate at 45 h APF, as detected by ligation to global expression of sDogCatcher-6xGFP. A single confocal slice is shown as merged (*C*), GFP Only (*C*′), and CHP only (*C*″) images. (*D* and *D*′) Magnified labeling of homozygous DIP-α-DogTag at endogenous levels in the medulla at 45 h APF. Distinct protein localization can be seen in M1, M3, and one additional layer in the distal medulla, as well as labeling of one proximal medulla layer. A single confocal slice is shown as merged (*D*) and GFP only (*D*′) images. Pink and blue arrowheads (*D*′) correspond to M1 layer (Dm1) and M3 layer (Dm4, Dm12), respectively. (*E*, *E*′, and *E*″) Heat shock-induced sDogCatcher-6xGFP expression with wildtype DIP-α and Dpr10 alleles shows no promiscuous labeling in the absence of DogTag at 27 h APF. (*F*, *F*′, and *F*″) Heat shock-induced sDogCatcher-6xGFP expression with wildtype DIP-α and Dpr10 alleles shows no promiscuous labeling in the absence of DogTag at 45 h APF. (*G*, *G*′, and *G*″) Homozygous Dpr10-DogTag expressed at endogenous levels localizes broadly across optic lobe neuropils at 27 h APF, as detected by ligation to global expression of sDogCatcher-6xGFP. A single confocal slice is shown as merged (*G*), GFP Only (*G*′), and CHP only (*G*″) images. (*H*, *H*′, and *H*″) Homozygous Dpr10-DogTag expressed at endogenous levels localizes to M1, M3, and other optic lobe neuropils at 45 h APF, as detected by ligation to global expression of sDogCatcher-6xGFP. A single confocal slice is shown as merged (*H*), GFP Only (*H*′), and CHP only (*H*″) images. (*I* and *I*′) Magnified labeling of homozygous Dpr10-DogTag at native levels in the medulla at 45 h APF. Distinct protein localization can be seen in M1 and M3 medullary layers. A single confocal slice is shown as merged (*I*) and GFP only (*I*′) images. Pink and blue arrowheads (*I*′) correspond to M1 layer (L5) and M3 layer (L3), respectively. *WT* = Wildtype proteins without DogTag. (All scale bars, 30 μm.) Me = Medulla. Lo = Lobula. Lop = Lobula plate. R8/R7 = R8/R7 photoreceptor terminals, respectively.

Dpr10-L298-DogTag, Dpr10-A313-DogTag, mCD8-S151-DogTag, mCD8-T169-DogTag, and mCD8-R181-DogTag), failed to produce notable increases in fluorescent signal, suggesting that they were unable to be productively bound by DogCatcher (*SI Appendix*, Fig. S1 *A–F*). Instead, the best insertion sites were located in small loops within otherwise well-structured Ig-like domains. It is plausible that the structure of DogTag, which adopts a β hairpin conformation, may not be stable in unstructured protein environments, thus hindering DogTag-DogCatcher isopeptide bond formation (24). Based on our results, we suggest avoiding future DogTag insertions into large regions predicted to be unstructured.

We observed that overexpression of both DIP-α-DogTag and DIP-α-WT in larval muscles resulted in a complete loss of MNISN-1s innervation of m4, consistent with previous observations (17) and with the idea that interactions between DIP-α and Dpr10 in *cis* (in muscles) reduce the amount of endogenous Dpr10 available to interact with DIP-α in *trans*. Notably, *cis* inhibition by DIP-α and Dpr10 has also been observed in the adult leg neuromuscular system (20). The ability of DIP-α-DogTag to cause *cis* inhibition is one indication that the tag does not compromise its ability to interact with Dpr10. Further, animals homozygous for the *DIP-α-DogTag* or *dpr10-DogTag* alleles had normal MNISN-1s innervation frequency, both with and without ligation to sDogCatcher-6xGFP, suggesting that DogTag-DogCatcher chemistry and the covalent linking of fluorescent proteins in Ig2 does not interfere with the biophysical interaction required for their in vivo functions (Fig. 6*E*). Notably, when we expressed sDogCatcher-6xGFP globally to label CSPs, we were unable to distinguish whether covalent bond formation occurred as both proteins were moving through the secretory pathway or, alternatively, once the CSP reached the cell surface. In contrast, when sDogCatcher-6xGFP was expressed from cells that are distinct from those expressing the DogTagged protein, it is more likely that labeling occurred at the cell surface. Regardless, although global expression of sDogCatcher-6xGFP worked well for DIP-α-DogTag and Dpr10-DogTag, the ability to have both temporal and spatial control of sDogCatcher-6xGFP expression in vivo may be important for functional studies requiring extracellular-specific labeling and/or labeling in a temporally controlled manner.

At endogenous expression levels of Dpr10-DogTag, we observed protein labeling at the SSR enveloping both 1s and 1b boutons of m4, with stronger labeling at 1s boutons (Fig. 6*C*). Interestingly, the m4 1b motor neuron does not express any of the known Dpr10 binding partners (DIP-α, DIP-β, nor DIP-λ) (21, 37). We suggest that our ability to visualize Dpr10-DogTag at the 1b NMJ is a consequence of the more extensive SSR membrane enveloping the boutons of 1b compared to 1s, and that the higher signal at 1s boutons is a consequence of stabilization by a transsynaptic interaction with DIP-α (32, 46). Consistent with this idea, as with endogenously expressed Dpr10-DogTag, a stronger GFP signal at the 1s SSR was also observed when Dpr10-DogTag was overexpressed in larval muscles (Fig. 4*D*). In contrast, when mCD8-DogTag-mCherry, a molecule without known binding partners in *Drosophila*, was overexpressed in larval muscles and labeled by sDogCatcher-6xGFP, both the mCherry and GFP signals were stronger at the SSR of 1b compared to 1s (Fig. 4*F*), consistent with previous observations (47). These differences in signal intensity, in which mCD8-DogTag-mCherry localizes less strongly to the 1s SSR compared to Dpr10-DogTag, reinforces the idea that Dpr10-DogTag localization, at both overexpressed and endogenous levels, is stabilized by its ability to interact with DIP-α.

In addition to endogenous labeling at single-cell resolution in both the larval and adult neuromuscular junctions, FETCH achieved population-level protein-specific labeling in the medulla neuropil and central brain. Taken together, these experiments demonstrate the broad applicability of this technique for the visualization of proteins in vivo in different tissues at different developmental stages. Finally, we suggest that DogTag-DogCatcher technology has the potential for many additional in vivo applications beyond fluorescent labeling, in both invertebrate and vertebrate experimental systems. We envision that covalent interaction between DogTag and DogCatcher variants could also be used to force protein interactions across synapses, induce protein-specific degradation or proximity labeling, and visualize protein dynamics in live animals.

Materials and Methods

Cloning of DogTag and DogCatcher Constructs. Synthesized Isoform A exon variants of DIP-α (UniProt ID: Q9W4R3) and Dpr10 (UniProt ID: Q9VT83) were used as template in the generation of DogTag DIP-Dpr variants (GenScript). pUAST-mCD8-GFP (Addgene #17746), encoding mouse CD8 subunit alpha, served as template for the generation of mCD8-DogTag variants. DogTag candidates for each CSP were then subcloned into a bicistronic mammalian expression vector containing an internal ribosome entry site (IRES) for flow cytometry. Transfection into HEK293 Freestyle cells resulted in the transcription of a single mRNA achieving DogTag-CSP expression from translation of the first cistron, whereas translation of the second cistron would result in cytoplasmic mCherry reporter expression, serving as both a marker of transfection efficiency and a correlate of DogTag-CSP expression levels. For biochemistry, extracellular domain fragments of CSPs with DogTag insertions were adapted with a hemagglutinin (HA) signal peptide and C-terminal SpyTag003 and 8xHis-Tag through cloning into a CMV promoter-bearing mammalian expression vector. DogTag-CSPs and recombinant DogCatcher-moxGFP variants were cloned into plasmids containing attB sites for integration into the *Drosophila* genome through site-specific integration. pJ404-DogCatcher-sfGFP (Addgene #171930) served as template for the amplification of the 104-amino acid DogCatcher protein, and moxGFP (Addgene #68070) served as template for the amplification of moxGFP. DogTag was introduced into protein loops through overlap extension PCR. See *SI Appendix*, Tables S4–S6 and S9 for cloning procedures.

Tissue Culture and Transient Transfection. HEK293 Freestyle suspension cells were cultured in HEK Freestyle Media (Invitrogen, 12338018) and grown at 37 °C in a humidified shaking platform incubator with 10% CO_2. For transfection, cells were pelleted at 500×*g* and resuspended in fresh media. For small-scale (1 mL cells at 1 × 10^6/mL) transient transfections performed in 24-well nontreated tissue culture plates, 10 μL of 293Fectin (ThermoFisher, 12347019) was added to 330 μL of Opti-MEM (ThermoFisher, 31985062), and incubated for 5 min at room temperature. Then, 10 μl of transfection mixture was added to 1 μg of DNA, and incubated at room temperature for 30 min, after which it was added to HEK293 Freestyle cells in 24-well plates.

Flow Cytometry Analysis of DogTag/DogCatcher Covalent Bond Formation. Flow cytometry titration assays were performed with cells expressing wildtype and DogTag variants of DIP-α, Dpr10, mCD8-mCherry, and sDogCatcher-GFP, transfected as described above. One day post transfection, cells were counted and diluted to 1 × 10^6 cells/mL in 1xPBS 0.2% BSA, pH 7.4. Cells transfected with sDogCatcher-GFP were spun down at 500×*g* for 2 min and supernatant was collected. Supernatant was then spun down at 2000×*g* for 5 min to remove debris, and supernatant was collected again. Then, 50 μL of cells expressing DogTag variants of DIP-a, Dpr10, and mCD8 were added to 96-well plates (ThermoFisher, 262162) and combined with 50 μL of DogCatcher-GFP supernatant. Then, 96-well plates were incubated on an Elexa E5 Platform Shaker (New Brunswick Scientific) shaking at 250 rpm for 60 min at room temperature. Cells were then washed twice by centrifugation and removal of supernatant, and resuspending in 1xPBS 0.2% BSA. Cells were then analyzed by flow cytometry on a Novocyte Quanteon (Agilent). Gated live cells were subgated for high mCherry expression, and then subgated for GFP intensity. Analysis of flow data was done in FlowJo (FlowJo LLC).

Transfection and Purification of Soluble Proteins. Expi293 suspension cells (ThermoFisher, A41249) were cultured in Expi293 medium (ThermoFisher, A1435101) and grown at 37 °C in a humidified shaking platform incubator at 130 rpm with 8% CO_2. For transfection, cells were introduced into prewarmed Expi293 medium at a concentration of 3 × 10^6 cells/mL. In two separate tubes, 50 μL of Opti-MEM (ThermoFisher, 31985062) per 1 mL transfection was prepared. Then, 1 μg of plasmid DNA per 1 mL transfection was added to the first tube; 2.7 μL ExpiFectamine 293 Reagent (ThermoFisher, A14525) per 1 mL transfection was added to the second tube and mixed before incubation at room temperature for 3 min. DNA and ExpiFectamine tube contents were mixed and incubated at room temperature for 5 min. The mixture was then added to Expi293 cells and shaken at aforementioned conditions. After 16 to 20 h, ExpiFectamine 293 Transfection Enhancers 1 and 2 (ThermoFisher, A14525) were added to cells at 5 μL and 50 μL per 1 mL of transfection, respectively. After 96 h, cells were pelleted at 4,000 rpm for 15 min at 4 °C. Supernatant was loaded through a 1 mL HisTrap FF column (Cytiva Life Sciences, 17531901) at 0.5 mL/min using a peristaltic pump. The

column was washed with 10 mL of 20 mM imidazole (ThermoFisher, A10221) in 1xPBS. Protein was eluted with 5 mL of 250 mM imidazole in 1xPBS.

Coupling Reactions. Purified proteins were kept at −80 °C for long term storage. Small aliquots were kept at 4 °C for immediate experimental use. For Dpr10-DogTag-SpyTag003-8xHis and mCD8-DogTag-SpyTag003-8xHis, protein amount was constant at 5 pmols across all ligation experiments. For both DogCatcher-GFP and SpyCatcher003, protein amounts of 2.5 pmols, 5 pmols, and 10 pmols were used in independent coupling reactions with 5 pmols of the aforementioned tagged extracellular domain fragments. For DIP-α-DogTag-SpyTag003-8xHis, protein amount was constant at 2.5 pmols across these ligation experiments. DogCatcher-GFP and SpyCatcher003 protein amounts of 1.25 pmols, 2.5 pmols, and 5 pmols were used in independent coupling reactions with 2.5 pmols of this tagged extracellular domain fragment. For all coupling reactions, proteins were incubated together in 8-strip PCR tubes at room temperature in 1xPBS (pH 7.4) for 1 h in a total volume of 10 μL. For all experiments, proteins were also ran alone at aforementioned amounts and subjected to conditions identical to those for coupling.

SDS-PAGE Analysis. Purified protein was concentrated further through 10 kDa MWCO Ultra Centrifugal Filter (Millipore, UFC9010). 4xSDS-PAGE loading dye with 10% β-mercaptoethanol was added to samples before a 10 min incubation at 98 °C. Proteins were run on 12-well precast protein gels (Bio-Rad, 4561085) with BSA standards (ThermoFisher, 23208) to obtain protein concentrations. For all coupling reactions, proteins were incubated in a total volume of 10 μL. Then, 3.33 μL 4xSDS-PAGE loading dye with 10% β-mercaptoethanol was added to samples and incubated for 10 min at 98 °C. Proteins were then run on 15-well precast protein gels (Bio-Rad, 4651086). Gels were stained with Coomassie InstantBlue (Abcam, ab119211) and imaged with a ChemiDoc XRS+ molecular imager (Bio-Rad).

Transgenesis. All plasmids for site-specific recombination and introduction into the *Drosophila* genome carried *attB* sites. *Enhancer-Flp* constructs were injected into *attP40w-* flies (Rainbow Transgenic Flies). UAS expression constructs of tagged and wildtype CSPs (DIP-α, Dpr10, and mCD8-mCherry) were injected into *attP2w-* flies (Rainbow Transgenic Flies). sDogCatcher-GFP constructs were injected into *attP1w-* flies (Rainbow Transgenic Flies). See *SI Appendix*, Tables S3–S5, S7 and S8 for detailed cloning procedures.

Generation of *DIP-α-DogTag* and *Dpr10-DogTag* CRISPR Alleles. We chose protospacer sequences in the exon regions of DIP-α and Dpr10 to insert DogTag after Ser148 and Ser261, respectively. DogTag insertions were flanked with GGGGS for DIP-α and GGGS for Dpr10. High score protospacer sequences were chosen on http://crispr.dfci.harvard.edu/SSC/. We cloned independent protospacers into pCFD3-dU6:3gRNA (Addgene #49410) and coinjected the plasmid and single-stranded repair template (Integrated DNA Technologies) into CAS0001 flies (Rainbow Transgenic Flies). Injected embryos were crossed to balancer lines, and F1 individuals were PCR screened for successful mutagenesis. Stable stocks were established from individuals demonstrating successful DogTag insertion and correct genomic repair. sgRNA and ssODN sequences are below. Detailed protocols available upon request.

DIP-α-DogTag sgRNA: TCCGCCGGACTTCATCAGCG

DIP-α-DogTag ssODN (5′ to 3′): CGCACGGAACTGCCCTCCGGCACAATCACATCGGATGA GGTGTCCTCGGAACCACCGCCGCCTTTCGGCGGTATCGGTTCATTGGTGATATAATGTTTACCATCGGTGAATTCGTATGTAGCCGGAATATCCGAGCCGCCTCCTCCGCTGATGAAGTCCGGCGGAATCACGACGTCCAGGAAGCCAATCTACAATTACC

Dpr10-DogTag sgRNA: ATTCAAGACCATCAAGTCGG

Dpr10-DogTag ssODN (5′ to 3′): CAGAGTGCAGGAGATCCGCATCGTAAATGAGCAAAATG GATTTGGTCTCCTCGGAACCGCCGCCTTTCGGCGGTATCGGTTCATTGGTGATATAATGTTTACCATCGGTGAATTCGTATGTAGCCGGAATATCCGAGCCTCCTCCCGACTTGATGGTCTTGAATTTCAGTCGGCCGCCCGAAGTTTCCTCGCTGAGCACC

Dissections. Larval fillets were dissected in cold 1xPBS and fixed for 25 min with 4% PFA in 1xPBS. Fillets were washed 4× for 10 min in 1xPBS, and then 3× for 10 min in cold PBST-BSA (0.05% Triton, 0.1% BSA) on a nutator at room temperature. PBST-BSA was replaced with 5% heat-inactivated normal goat serum (Gibco, 16210064) in PBST-BSA and blocked overnight on a nutator at 4 °C. Alexa Fluor 647-conjugated goat antihorseradish peroxidase (Jackson ImmunoResearch, 123605021; 1:100) was incubated with filets in 5% HI-NGS in PBST-BSA overnight on a nutator at 4 °C. Fillets were then washed 4× for 10 min with PBST-BSA and 2× for 10 min with 1xPBS on nutator at room temperature. Samples were then placed ventral side downward and mounted in Vectashield (Vector Laboratories, H100010). For adult leg dissections, flies were immersed in 70% ethanol for 30 s and rinsed 3× in PBST (0.3% Triton). Abdomen and heads were removed and legs still attached to thoracic segments were fixed with 4% PFA-PBST overnight on a nutator at 4 °C. Then, legs and thorax were washed 5× in PBST and stored overnight in 80% mounting medium (Vector Laboratories, H100010) in 1xPBS overnight at 4 °C. T1 legs were then removed from thoracic segments and mounted with dental wax on the corners of coverslips to accommodate leg thickness. For optic lobe and central brain samples, prepupae or pupae of the appropriate genotype were collected at 0 h or 20 h APF, given heat-shock for 30 min, and aged until either 27 h or 45 h APF, respectively. Brains were then dissected and stained according to previously described immunohistochemistry protocols (7). No experiments included sDogCatcher-6xGFP signal amplification except for *SI Appendix*, Fig. S5. See *SI Appendix*, Tables S1 and S2 for heat shock conditions and genetic reagents.

Microscopy. A Zeiss Axio Imager 2 based LSM800 confocal laser scanning microscope with a 63×/1.4 NA oil-immersion objective was used for imaging single slices for larval and adult neuromuscular junctions. A 25×/0.8 NA oil-immersion objective was used for imaging larval VNCs with a step size of 0.5 μm. A 10×/0.3 NA nonconfocal objective was used for imaging wing imaginal discs and pupae with step sizes of 0.5 μm and 1.0 μm, respectively. A Zeiss LSM980 confocal laser scanning microscope with a 40×/1.4NA oil-immersion objective was used for imaging optic lobe and central brain samples with a step size of 0.8 μm. Laser power and gain settings were identical across samples in each set of experiments. Post image processing was identical across samples in each set of experiments and performed with ImageJ software.

Statistical Analysis. Analysis of innervation frequency was performed with GraphPad Prism 10.1.0 software (San Diego, CA). MNISN-1s innervation of third instar larval muscle 4 was quantified as either present (1) or absent (0), with values across hemisegments averaged per animal. Statistical analysis for significance between conditions was evaluated with an unpaired, nonparametric Mann–Whitney *U* test.

Data, Materials, and Software Availability. All study data are included in the article and/or *SI Appendix*.

ACKNOWLEDGMENTS. This work was supported by NIH Grants R01 NS070644 and R35 GM118336 to R.S.M., NSF Grant IOS-2321481 to K.Z. and L.S, and predoctoral training grant 5T32GM141882. We thank William J. Glassford for input in designing the Dpr10-DogTag CRISPR allele. We thank Michael Anaya and Annie W. Lam for assistance with mammalian expression and purification of proteins for biochemistry experiments. We thank Frank Schnorrer for providing details for the *Him* enhancer, Gary Struhl for sharing *hh-Gal4* reagents and stop cassette DNA, Anina Young for fly husbandry, Alina P. Sergeeva for discussions about DogTag insertions, and Jordan Becker for assisting with flow cytometry transfections. We thank all members of the Mann lab for discussions, and Chris Q. Doe for comments on the manuscript. We acknowledge the support of Columbia University's Summer Undergraduate Research Fellowship (SURF) program for supporting K.D.R. in the lab of R.S.M. in 2023 and the Amgen Foundation for supporting K.D.R. as an Amgen Scholar at the California Institute of Technology in the lab of K.Z. in 2024.

Author affiliations: [a]Department of Biochemistry and Molecular Biophysics, Vagelos College of Physicians and Surgeons, Columbia University, New York, NY 10032; [b]Mortimer B. Zuckerman Mind Brain Behavior Institute, Columbia University, New York, NY 10027; [c]Division of Biology and Biological Engineering, California Institute of Technology, Pasadena, CA 91125; [d]Aaron Diamond AIDS Research Center, Vagelos College of Physicians and Surgeons, Columbia University, New York, NY 10032; [e]Department of Genetics and Development, Vagelos College of Physicians and Surgeons, Columbia University, New York, NY 10027; [f]Department of Neuroscience, Vagelos College of Physicians and Surgeons, Columbia University, New York, NY 10032; and [g]Department of Systems Biology, Vagelos College of Physicians and Surgeons, Columbia University, New York, NY 10032

Author contributions: K.D.R., N.C.M., K.Z., S.F., and R.S.M. designed research; K.D.R., N.C.M., K.P.M., and D.H.L. performed research; K.D.R. contributed new reagents/analytic tools; K.D.R., N.C.M., K.P.M., L.S., and R.S.M. analyzed data; L.S., K.Z., and R.S.M. provided funding; K.D.R., N.C.M., K.P.M., and R.S.M. edited and revised the paper; and K.D.R. and R.S.M. wrote the paper.

1. M. Luis, S. Xu, K. Zinn, Fluorescent labeling of proteins in vitro and in vivo using encoded peptide tags. *J. Biol. Chem.* **301**, 110229 (2025).
2. M. Nakamura, D. Baldwin, S. Hannaford, J. Palka, C. Montell, Defective proboscis extension response (DPR), a member of the Ig superfamily required for the gustatory response to salt. *J. Neurosci.* **22**, 3463–3472 (2002).
3. E. Özkan *et al.*, An extracellular interactome of immunoglobulin and LRR proteins reveals receptor-ligand networks. *Cell* **154**, 228–239 (2013).
4. S. Cheng *et al.*, Molecular basis of synaptic specificity by immunoglobulin superfamily receptors in *Drosophila*. *eLife* **8**, e41028 (2019).
5. A. P. Sergeeva *et al.*, DIP/Dpr interactions and the evolutionary design of specificity in protein families. *Nat. Commun.* **11**, 2125 (2020).
6. L. Tan *et al.*, Ig superfamily ligand and receptor pairs expressed in synaptic partners in *Drosophila*. *Cell* **163**, 1756–1769 (2015).
7. K. P. Menon, V. Kulkarni, S. Takemura, M. Anaya, K. Zinn, Interactions between Dpr11 and DIP-γ control selection of amacrine neurons in *Drosophila* color vision circuits. *eLife* **8**, e48935 (2019).
8. S. Barish *et al.*, Combinations of DIPs and Dprs control organization of olfactory receptor neuron terminals in *Drosophila*. *PLoS Genet.* **14**, e1007560 (2018).
9. R. A. Carrillo *et al.*, Control of synaptic connectivity by a network of *Drosophila* IgSF cell surface proteins. *Cell* **163**, 1770–1782 (2015).
10. S. G. Brovero *et al.*, Investigation of *Drosophila* fruitless neurons that express Dpr/DIP cell adhesion molecules. *eLife* **10**, e63101 (2021).
11. C. Xu *et al.*, Control of synaptic specificity by establishing a relative preference for synaptic partners. *Neuron* **103**, 865–877.e7 (2019).
12. P. Nandigrami *et al.*, Computational assessment of protein–protein binding specificity within a family of synaptic surface receptors. *J. Phys. Chem. B* **126**, 7510–7527 (2022).
13. J. R. Sanes, S. L. Zipursky, Synaptic specificity, recognition molecules, and assembly of neural circuits. *Cell* **181**, 536–556 (2020).
14. M. Courgeon, C. Desplan, Coordination between stochastic and deterministic specification in the *Drosophila* visual system. *Science* **366**, eaay6727 (2019).
15. S. Xu *et al.*, Interactions between the Ig-superfamily proteins DIP-α and Dpr6/10 regulate assembly of neural circuits. *Neuron* **100**, 1369–1384.e6 (2018).
16. S. Xu *et al.*, Affinity requirements for control of synaptic targeting and neuronal cell survival by heterophilic IgSF cell adhesion molecules. *Cell Rep.* **39**, 110618 (2022).
17. J. Ashley *et al.*, Transsynaptic interactions between IgSF proteins DIP-α and Dpr10 are required for motor neuron targeting specificity. *eLife* **8**, e42690 (2019).
18. L. Venkatasubramanian *et al.*, Stereotyped terminal axon branching of leg motor neurons mediated by IgSF proteins DIP-α and Dpr10. *eLife* **8**, e42692 (2019).
19. D. H. Lopez, K. D. Rostam, S. Zamurrad, S. Xu, R. S. Mann, A critical affinity window for IgSF proteins DIP-α and Dpr10 is required for proper motor neuron arborization. *Genes Dev.* (2025).
20. N. C. Morano *et al.*, Members of the DIP and Dpr adhesion protein families use cis inhibition to shape neural development in *Drosophila*. *PLoS Biology* 23, e3003030 (2025).
21. F. Cosmanescu *et al.*, Neuron-subtype-specific expression, interaction affinities, and specificity determinants of DIP/Dpr cell recognition proteins. *Neuron* **100**, 1385–1400.e6 (2018).
22. M. Lobb-Rabe *et al.*, Neuronal wiring receptors Dprs and DIPs are GPI anchored and this modification contributes to their cell surface organization. *ENeuro* **11**, ENEURO.0184-23.2023 (2024).
23. K. Zhou, Glycosylphosphatidylinositol-anchored proteins in Arabidopsis and one of their common roles in signaling transduction. *Front. Plant Sci.* **10**, 1022 (2019).
24. A. H. Keeble *et al.*, Dogcatcher allows loop-friendly protein–protein ligation. *Cell Chem. Biol.* **29**, 339–350.e10 (2022).
25. S. Feng, R. S. Mann, Spychip identifies cell type-specific transcription factor occupancy from complex tissues. *Proc. Natl. Acad. Sci. U.S.A.* **119**, e2122900119 (2022).
26. T. Lee, L. Luo, Mosaic analysis with a repressible cell marker for studies of gene function in neuronal morphogenesis. *Neuron* **22**, 451–461 (1999).
27. H.-C. Chang *et al.*, Structural and mutational analyses of a CD8αβ heterodimer and comparison with the CD8αα homodimer. *Immunity* **23**, 661–671 (2005).
28. J. Abramson *et al.*, Accurate structure prediction of biomolecular interactions with AlphaFold 3. *Nature* **630**, 493–500 (2024).
29. L. M. Costantini *et al.*, A palette of fluorescent proteins optimized for diverse cellular environments. *Nat. Commun.* **6**, 7670 (2015).
30. S. Barash, W. Wang, Y. Shi, Human secretory signal peptide description by hidden Markov model and generation of a strong artificial signal peptide for secreted protein expression. *Biochem. Biophys. Res. Commun.* **294**, 835–842 (2002).
31. A. H. Keeble *et al.*, Approaching infinite affinity through engineering of peptide–protein interaction. *Proc. Natl. Acad. Sci.* **116**, 26523–26533 (2019).
32. K. P. Menon, R. A. Carrillo, K. Zinn, Development and plasticity of the *Drosophila* larval neuromuscular junction. *WIREs Dev. Biol.* **2**, 647–670 (2013).
33. P. Klein *et al.*, Ret rescues mitochondrial morphology and muscle degeneration of *Drosophila Pink1* mutants. *EMBO J.* **33**, 341–355 (2014).
34. A. A. Lazareva, G. Roman, W. Mattox, P. E. Hardin, B. Dauwalder, A role for the adult fat body in *Drosophila* male courtship behavior. *PLoS Genet.* **3**, e16 (2007).
35. M. Silies *et al.*, Glial cell migration in the eye disc. *J. Neurosci.* **27**, 13130–13139 (2007).
36. H. Asha *et al.*, Analysis of Ras-induced overproliferation in *Drosophila* hemocytes. *Genetics* **163**, 203–215 (2003).
37. Y. Wang *et al.*, Systematic expression profiling of Dpr and DIP genes reveals cell surface codes in Drosophila larval motor and sensory neurons. *Development* **149**, dev200355 (2022).
38. A. Nern, B. D. Pfeiffer, G. M. Rubin, Optimized tools for multicolor stochastic labeling reveal diverse stereotyped cell arrangements in the fly visual system. *Proc. Natl. Acad. Sci.* **112**, E2967–E2976 (2015).
39. C.-Y. Ting *et al.*, *Drosophila* N-cadherin functions in the first stage of the two-stage layer-selection process of R7 photoreceptor afferents. *Development* **132**, 953–963 (2005).
40. T. Wolff, N. A. Iyer, G. M. Rubin, Neuroarchitecture and neuroanatomy of the Drosophila central complex: A GAL4-based dissection of protocerebral bridge neurons and circuits. *J. Comp. Neurol.* **523**, 997–1037 (2015).
41. R. Kamiyama *et al.*, Cell-type–specific, multicolor labeling of endogenous proteins with split fluorescent protein tags in *Drosophila*. *Proc. Natl. Acad. Sci. U.S.A.* **118**, e2024690118 (2021).
42. J. Xu *et al.*, Protein visualization and manipulation in *Drosophila* through the use of epitope tags recognized by nanobodies. *eLife* **11**, e74326 (2022).
43. G. Aguilar *et al.*, Seamless knockins in *Drosophila* via CRISPR-triggered single-strand annealing. *Dev. Cell* **59**, 2672–2686.e5 (2024).
44. S. Fendl, R. M. Vieira, A. Borst, Conditional protein tagging methods reveal highly specific subcellular distribution of ion channels in motion-sensing neurons. *eLife* **9**, e62953 (2020).
45. P. Sanfilippo *et al.*, Mapping of multiple neurotransmitter receptor subtypes and distinct protein complexes to the connectome. *Neuron* **112**, 942–958.e13 (2024).
46. T. Lahey, M. Gorczyca, X.-X. Jia, V. Budnik, The *Drosophila* tumor suppressor gene dlg is required for normal synaptic bouton structure. *Neuron* **13**, 823–835 (1994).
47. K. Zito, R. D. Fetter, C. S. Goodman, E. Y. Isacoff, Synaptic clustering of Fasciclin II and Shaker: Essential targeting sequences and role of Dlg. *Neuron* **19**, 1007–1016 (1997).